Journal of Controlled Release 375 (2024) 767–775

Contents lists available at ScienceDirect

Journal of Controlled Release

journal homepage: www.elsevier.com/locate/jconrel

PSMA and Sigma-1 receptor dual-targeted peptide mediates superior radionuclide imaging and therapy of prostate cancer

Zhenyuan Huangfu [a,b,1], Jiangtao Yang [a,b,1], Juan Sun [a,b,1], Bin Xu [a,b], Lei Tao [a,b], Jiang Wu [c], Feng Wang [c,**], Guanglin Wang [d,**], Fenghua Meng [a,b], Zhiyuan Zhong [a,b,*]

[a] Biomedical Polymers Laboratory, College of Chemistry, Chemical Engineering and Materials Science, and State Key Laboratory of Radiation Medicine and Protection, Soochow University, Suzhou 215123, People's Republic of China
[b] College of Pharmaceutical Sciences, Soochow University, Suzhou 215123, People's Republic of China
[c] Department of Nuclear Medicine, Nanjing First Hospital, Nanjing Medical University, Nanjing 210006, People's Republic of China
[d] State Key Laboratory of Radiation Medicine and Protection, School of Radiation Medicine and Protection, Collaborative Innovation Center of Radiological Medicine of Jiangsu Higher Education Institutions, Soochow University, Suzhou 215123, China

ARTICLE INFO

Keywords:
Peptides
Targeted delivery
Prostate cancer
Theranostics
Radionuclide therapy

ABSTRACT

Radionuclide therapy, in particular peptide receptor radionuclide therapy (PRRT), has emerged as a valuable means to combat malignant tumors. The specific affinity of ACUPA peptide toward prostate-specific membrane antigen (PSMA) renders the successful development of PRRT for prostate cancer. The clinical outcome of PRRT is, however, generally challenged by moderate tumor uptake and off-target toxicity. Here, we report on a novel design of Sigma-1 receptor and PSMA dual-receptor targeted peptide (S1R/PSMA-P) for superior radionuclide imaging and therapy of prostate cancer. S1R/PSMA-P was acquired with good purity and could efficiently be labeled with ^{177}Lu to yield ^{177}Lu-S1R/PSMA-P with high specific activity and radiostability. Interestingly, ^{177}Lu-S1R/PSMA-P revealed greatly enhanced affinity to LNCaP cells over single-targeted control ^{177}Lu-PSMA-617. The single photon emission computed tomography (SPECT) imaging demonstrated exceptional uptake and retention of ^{177}Lu-S1R/PSMA-P in LNCaP tumor, affording about 2-fold better tumor accumulation while largely reduced uptake by most normal tissues compared to ^{177}Lu-PSMA-617. The selective uptake in LNCaP tumor was also visualized by positron emission tomography (PET) with ^{68}Ga-S1R/PSMA-P. In accordance, a single and low dosage of ^{177}Lu-S1R/PSMA-P at 11.1 MBq effectively suppressed tumor growth without causing apparent side effects. This dual-targeting strategy presents an appealing radionuclide therapy for malignant tumors.

1. Introduction

Radionuclide therapy represents one of the most advanced precision therapies for malignant tumors [1–3]. Unlike common drugs such as chemotherapeutics and biotherapeutics, radionuclides cause DNA damage and thereby cell death by releasing high-energy particles such as alpha and beta particles [4]. Certain radionuclides such as ^{177}Lu can release gamma and beta particles, which render it suitable for both imaging and therapy [5]. It is also possible to integrate diagnosis and treatment by replacing therapeutic radionuclides (e.g. ^{177}Lu) with diagnostic radionuclides (e.g. ^{68}Ga), thereby achieving theranostics with exactly the same ligand [6–8]. Peptide receptor radionuclide therapy (PRRT) is on the frontier of radionuclide therapy [9–11]. The efficacy of PRRT in the treatment of malignant tumors has been clinically validated, particularly when targeting highly expressed receptors such as the overexpressed prostate-specific membrane antigen (PSMA) receptor of prostate cancer and somatostatin receptor of neuroendocrine tumors [12–15]. ^{177}Lu-DOTA-TATE (Lutathera) and ^{177}Lu-PSMA-617 (Pluvicto) were granted approval by the authority in 2018 and 2022, respectively [16]. PSMA-targeted PRRT is widely recognized as an effective treatment for metastatic castration-resistant prostate cancer (mCRPC) [16–18]. Of note, the tumor uptake and retention as well as safety of

* Corresponding author at: Biomedical Polymers Laboratory, College of Chemistry, Chemical Engineering and Materials Science, and State Key Laboratory of Radiation Medicine and Protection, Soochow University, Suzhou 215123, People's Republic of China.
** Corresponding authors.
E-mail addresses: fengwangcn@hotmail.com (F. Wang), glwang@suda.edu.cn (G. Wang), zyzhong@suda.edu.cn (Z. Zhong).
[1] These authors have made equal contribution.

https://doi.org/10.1016/j.jconrel.2024.09.040
Received 19 June 2024; Received in revised form 26 August 2024; Accepted 23 September 2024
Available online 2 October 2024

PRRT still present significant opportunities for improvement [19,20].

A variety of approaches involving the structural modification of PSMA-targeting urea molecules are currently being investigated in depth with the goal of enhancing the efficacy of ^{177}Lu-PSMA-617. Molecules designed to contain functional groups that non-covalently bind to serum albumin, such as 4-(para-iodophenyl) butyric acid, truncated Evans blue, ibuprofen, and fatty acids, have been reported with the most frequency [21–25]. These molecules are designed to increase circulation time, thereby increasing tumor uptake and reducing the administered dose. Nevertheless, a prolonged circulation time while resulting in an increased tumor uptake is also accompanied by significantly enhanced distribution in healthy organs. This, in turn, leads to decrease rather than increase of tumor-selectivity and accordingly increase of off-target toxicity [26–28]. Another strategy for modifying the pharmacokinetics is to alter the ligand's hydrophilicity. This can be achieved by the introduction of a polyethylene glycol (PEG) molecule between the Lys-Urea-Glu and the chelator [29–32]. The introduction of PEG facilitates renal excretion of the ligand, thereby reducing the toxicity of PRRT to the blood and kidneys [33]. Nevertheless, there was no augmentation or even reduction of tumor accumulation.

Dual and multiple targeting ligands have shown interesting features such as higher tumor uptake, improved tumor-to-normal tissue ratio, and prolonged tumor retention [34,35]. For instance, the combination of a PSMA ligand with a targeting ligand for gastrin-releasing peptide receptors (GRPR) or fibroblast activation protein (FAP) resulted in the creation of new ligands with enhanced tumor uptake and retention, enabling imaging of metastatic foci and tumors with a low PSMA expression [36–40]. GRPR is highly expressed in the early stages of prostate cancer, while FAP is expressed on fibroblasts rather than the tumor cell itself. The Sigma-1 receptor, also known as Sigma-1, is a transmembrane protein that plays a role in a number of biological processes, including neurodegenerative disorders and cancer [41–43]. Its overexpression has been observed in more than 40 % of prostate cancer patients [44,45]. PET imaging of Sigma-1 receptor has been

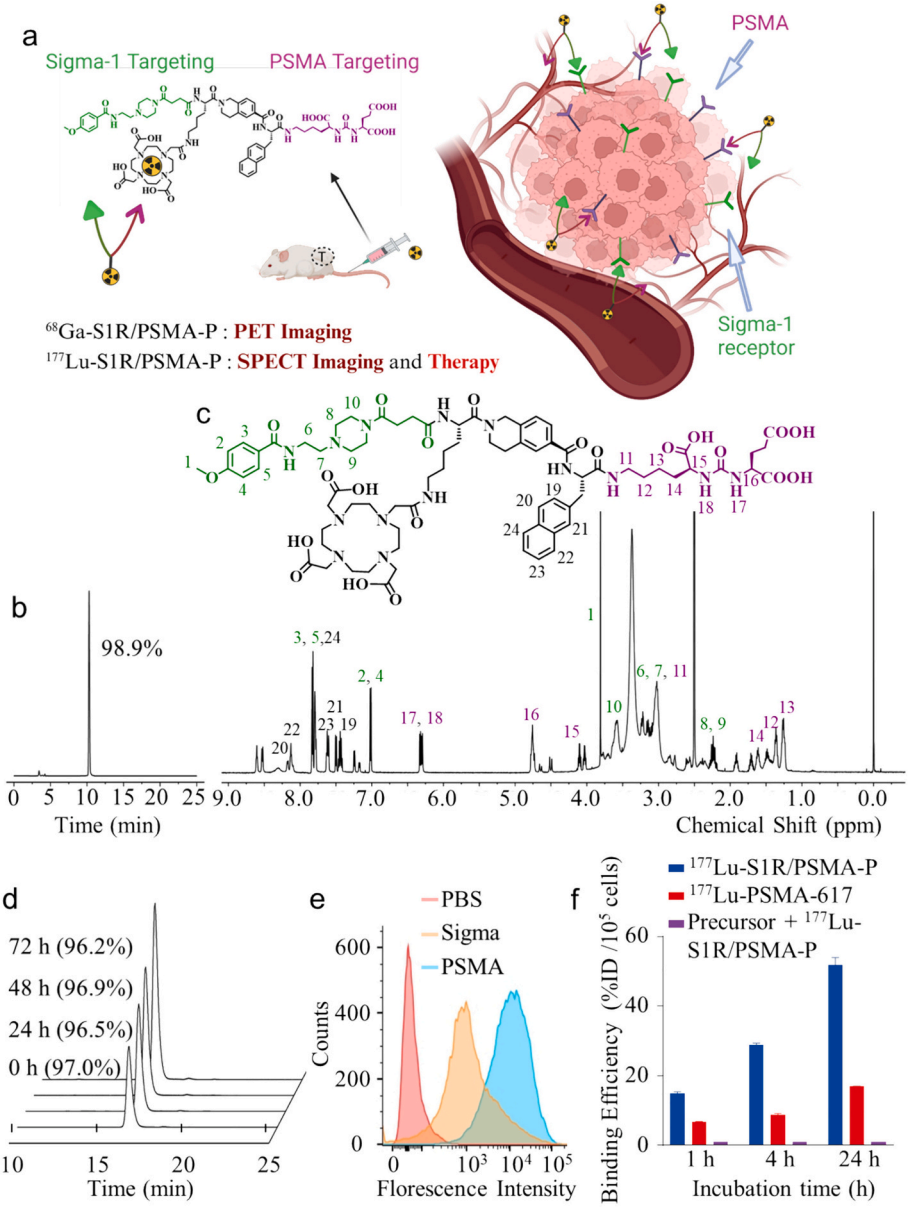

Fig. 1. (a) Schematic drawing of ^{68}Ga/^{177}Lu-S1R/PSMA-P for dually targeted radionuclide imaging and therapy of prostate cancer. (b) The purity of S1R/PSMA-P analyzed by HPLC. (c) ^{1}H NMR spectrum of S1R/PSMA-P in DMSO-d_6. (d) The radio-purity of ^{177}Lu-S1R/PSMA-P in PBS at room temperature over time analyzed by HPLC. (e) The expression of Sigma receptor and PSMA in LNCaP cells by flow cytometry. (f) Binding efficiency of ^{177}Lu-S1R/PSMA-P to LNCaP cells at varying times from 1 h to 24 h. ^{177}Lu-PSMA-617 was used as a control. The competitive experiments were carried out in the presence of 6.5 mM free S1R/PSMA-P.

explored in the clinic for imaging the origin of pain [46]. Subsequent to its initial discovery, a number of ligands such as anisamide have been developed to target Sigma-1 receptor, and radiolabelled anisamide and its derivatives, as well as anisamide-modified nanomedicines, have been extensively studied for tumor diagnosis and therapy [47–50].

The objective of this study was to design a novel dual-receptor targeted ligand that specifically binds to both Sigma-1 receptor and PSMA, designated as S1R/PSMA-P, for enhanced radionuclide imaging and therapy of prostate cancer (Fig. 1a). S1R/PSMA-P containing anisamide and ACUPA peptide can be stably radiolabeled with ^{177}Lu and ^{68}Ga. The single photon emission computed tomography (SPECT) demonstrated superior selectivity, uptake and retention of ^{177}Lu-S1R/PSMA-P in LNCaP tumor to single targeted control (^{177}Lu-PSMA-617). The positron emission tomography (PET) confirmed selective uptake of ^{68}Ga-S1R/PSMA-P by LNCaP tumor. Notably, a single dose of ^{177}Lu-S1R/PSMA-P at 11.1 MBq was shown to effectively suppress tumor growth, significantly outperforming single PSMA-targeted control at 33.3 MBq. S1R/PSMA-P appears to be an interesting ligand for high-efficacy theranostics of prostate cancer.

2. Experimental

2.1. Materials

All chemicals were purchased commercially. $^{177}LuCl_3$ and ^{68}Ge—^{68}Ga generator were purchased from China Isotope & Radiation Corporation with a radionuclide purity of >99 %. S1R/PSMA-P was synthesized by BioAct Peptide Biotechnology LLC. S1R/PSMA-P was characterized by mass spectrometry (MS) and nuclear magnetic resonance spectroscopy (^{1}H NMR). ^{1}H NMR (600 MHz, DMSO-d_6):δ 8.61–8.59 (t, 1H), 8.53–8.52 (d, 1H), 8.18–8.10 (m, 2H), 7.84–7.78 (m, 5H), 7.63–7.60 (m, 2H), 7.51–7.49 (m, 1H), 7.47–7.41 (m, 2H), 7.25–7.24 (d, 1H), 7.18–7.17 (d, 1H), 7.03–7.00 (m, 2H), 6.33–6.29 (m, 2H), 4.78–4.73 (m, 3H), 4.52–4.49 (d, 1H), 4.12–4.08 (m, 1H), 4.05–4.01 (m, 1H), 3.81 (s, 3H), 3.78–3.58 (m, 12H), 3.24–3.00 (m, 26H), 2.89–2.77 (m, 4H), 2.61–2.56 (m, 2H), 2.44–2.18 (m, 6H), 1.95–1.89 (m, 2H), 1.74–1.67 (m, 2H), 1.63–1.59 (m, 2H), 1.51–1.42 (m, 3H), 1.38–1.34 (m, 3H), 1.28–1.23 (m, 4H). MS (m/z) $[M + H]^+$ $[C_{75}H_{103}N_{14}O_{21}]^+$ calculated = 1536.74, found 1536.37.

2.2. Radiosynthesis

S1R/PSMA-P was radiolabeled analogous to ^{177}Lu-PSMA-617 [29,35]. Briefly, 0.1 mmol of ligand was dissolved in 100 μL dimethyl sulfoxide (DMSO) and 0.4 M sodium acetate buffer at pH 4.5 with a final concentration of 0.2 mg/mL. A defined amount of ^{177}Lu was mixed with S1R/PSMA-P at a ratio of 1:6 and reacted at 95 °C for 15 min. The radiochemical yield and stability of ^{177}Lu-S1R/PSMA-P after incubating in PBS for 1 h to 72 h was determined by high-performance liquid chromatography (HPLC, Agilent). The mobile phase of the HPLC was set up with a Velch Xtimate C18 column (4.6 × 150 mm, 5 μm), 0.1 % H_3PO_4/water as mobile phase A, acetonitrile as mobile phase B at a flow rate of 1 mL/min. The gradient of mobile phase B, 0–20 min with 10 %–25 % B, 25–30 min with 25 %–90 % B, 30–32 min with 95 % B, and 32–40 min with 5 % B.

^{68}Ga was eluted from the organic column ^{68}Ge/^{68}Ga generator using 4 mL of 0.05 M HCl and immediately added to the reaction vessel containing 2.3 μg of S1R/PSMA-P dissolved in 23 μL of sodium acetate buffer (0.05 M, pH 4.5). The mixture was then reacted in a metal bath reactor at 95 °C for 15 min.

The purification steps for the reaction solution are as follows: activate the C18 column with 10 mL of 70 % ethanol solution, air dry, clean with 10 mL of normal saline, air dry, draw the reaction solution into the C18 column for purification, clean with 5 mL of normal saline, blow dry, and wash with 0.5 mL of 60 % ethanol. After purification, heat the ethanol to 95 °C to evaporate and redissolve it with 1 mL of normal saline (0.9 % NaCl). After heating, ^{68}Ga-S1R/PSMA-P was filtered through a 0.22 μm membrane filter for sterilization.

The radiochemical purity of ^{68}Ga-S1R/PSMA-P was determined using HPLC with Zorbax RaxC-18 (4.6 × 250 mm) column and a mobile phase consisting of acetonitrile solution containing 0.1 % TFA (A) and aqueous solution containing 0.1 % TFA (B). Gradient elution was performed at 1 mL/min, increasing from 5 % A and 95 % B in 2 min to 65 % A and 35 % B in 32 min. The radiochemical purity of ^{68}Ga-S1R/PSMA-P should be at least 95 %.

2.3. In vitro PSMA-binding assay

Human PSMA-positive LNCaP cells and mice PSMA-positive Sigma negative RM1 cells were cultured in DMEM (Gibco) and RPMI 1640 (HyClone) supplemented with 1 % penicillin, streptomycin (Kino Bio), and 10 % fetal bovine serum (FBS) (Gibco) at 37 °C and 5 % CO_2 in a Thermo Fisher Scientific incubator (Type 3111). In order to ascertain the binding and endocytosing ability of ^{177}Lu-S1R/PSMA-P to PSMA overexpressing cells, ^{177}Lu-S1R/PSMA-P or ^{177}Lu-PSMA-617 (5×10^5 counts per minute, CPM) were cultured with LNCaP cells in 24-well plates for 1, 4, and 24 h. At each designated time point, the medium was removed and the cells were washed three times with PBS. Subsequently, 0.2 mL of 1 M NaOH solution was added for the purpose of cell lysis. The lysate was then transferred to the release tube and the activity of each sample was measured using a gamma counter (PerkinElmer, Wallac 2480). In the blocking group, the precursor (S1R/PSMA-P, 0.1 mg) was added together with ^{177}Lu-S1R/PSMA-P, and the subsequent operations were conducted as mentioned above.

2.4. Imaging study

All animal experiments were approved by the Animal Care and Use Committee of Soochow University and conducted according to the Guidelines for the Care and Use of Experimental Animals. ^{177}Lu-S1R/PSMA-P and ^{177}Lu-PSMA-617 in PBS containing 0.5 % Tween 80 (7.4 MBq, 200 μL) were injected intravenously into LNCaP tumor-bearing mice (n = 3) and PC-3 tumor-bearing mice (n = 3) via the tail vein. Mice were anesthetized with isoflurane and whole-body imaged using *micro*SPECT/CT (Milabs, The Netherlands), with 5 min CT and 15 min SPECT scans at 1, 4, 8, 24, 48, and 72 h postinjection. The scanned data were reconstructed using U-SPECT-Rec2.51 g software and the distribution of ^{177}Lu-labeled ligands in the LNCaP tumor-bearing mice was quantitatively analyzed using PMOD software (Version 3.602).

PET/CT imaging was conducted on a Siemens Inveon small-animal PET/CT device. 3.7 MBq of ^{68}Ga-S1R/PSMA-P and ^{68}Ga-PSMA-617 in 200 μL of saline was intravenously injected into LNCaP tumor-bearing mice via the tail vein. The mice were anesthetized with isoflurane and placed on the scanner at 0.5, 1, and 2 h after administration. For the purpose of localization and attenuation correction, a CT scan was obtained using 80-kV tube voltage, 500 mA current, three bed positions, 34 % overlap, and 220° of continuous rotation. Subsequently, a 10 min PET acquisition was performed. The PET imaging data were acquired in list mode and subsequently reconstructed using a three-dimensional ordered-subsets expectation maximization algorithm with two iterations, followed by a fast maximum a priori algorithm with 18 iterations and CT-based attenuation correction. The images were analyzed using PMOD software (Version 3.602).

2.5. In vivo therapy

To assess the antitumor efficacy, LNCaP-FGC tumor-bearing mice were intravenously injected with PBS, varying doses of ^{177}Lu-S1R/PSMA-P from 3.7 MBq to 33.3 MBq, and 33.3 MBq of ^{177}Lu-PSMA-617 at the average tumor volume of 400 mm^3 (n = 10). Tumor volume and body weight were measured twice a week after administration.

2.6. Safety assessment of ^{177}Lu-S1R/PSMA-P

In order to assess the toxicity of ^{177}Lu-S1R/PSMA-P in healthy BALB/c mice, two groups of mice were administered either PBS or ^{177}Lu-S1R/PSMA-P at a dose of 7.4 MBq or 14.8 MBq via intravenous injection into the tail vein ($n = 5$). Blood samples were collected in anticoagulant tubes seven days after injection for analysis of blood cell, hemoglobin, and platelet counts levels.

To determine the tolerated dose of ^{177}Lu-S1R/PSMA-P, healthy BALB/c mice received PBS or 14.8 MBq, or 29.6 MBq of ^{177}Lu-S1R/PSMA-P by intravenous injection via the tail vein (n = 5). The body weight of the mice was recorded at 3-day intervals following the administration of the treatment. On 28th day following the injection, the major organs were harvested and sectioned. Each organ was then stained with hematoxylin and eosin (H&E).

In addition, a toxicity test was conducted on ^{177}Lu-S1R/PSMA-P in SD rats after tail vein injection at an extended single dose ($n = 10$). In accordance with the maximum dose of 7400 MBq (123.3 MBq/kg) for clinical preparation, a single dose of the drug equivalent to 8 times and 16 times the clinical activity dose was administered to SD male rats. Blood samples were collected in anticoagulant tubes four days after injection for analysis of blood cell and hemoglobin index level. The major organs were harvested and sectioned. Each organ was then stained with hematoxylin and eosin (H&E).

2.7. Statistical analysis

All data in this manuscript are presented as mean ± SD. Differences between groups were evaluated using one-way ANOVA and Tukey's post-hoc test. $p < 0.05$ was considered significant (*), < 0.01 (**) and < 0.001 (***) highly significant.

3. Results and discussion

3.1. Synthesis of S1R/PSMA-P and ^{177}Lu-S1R/PSMA-P

A novel dual-targeted ligand S1R/PSMA-P composed of ACUPA peptide and anisamide, which targets PSMA and Sigma-1 receptors, respectively, was designed to enhance tumor selectivity and uptake. The synthesis of S1R/PSMA-P is illustrated in **Fig. S1**. The purity of S1R/PSMA-P as analyzed by HPLC was greater than 95 % (Fig. 1b). ^{1}H NMR spectrum of S1R/PSMA-P in DMSO-d_6 corroborated the chemical structure of S1R/PSMA-P (Fig. 1c). The mass spectrum displayed an m/z $[M + H]^+$ of 1536.37 (**Fig. S2**), corresponding to the theoretical mass of S1R/PSMA-P. These results demonstrated the successful synthesis of S1R/PSMA-P.

S1R/PSMA-P could easily be labeled with ^{177}Lu. The radiochemical yield of ^{177}Lu-S1R/PSMA-P exceeded 97 % in acetate buffer (pH 4.5) as determined by radio-HPLC. The specific activity of ^{177}Lu-S1R/PSMA-P was calculated to be 49.3 MBq/nmol. Fig. 1d shows that ^{77}Lu-S1R/PSMA-P had excellent radiostability in PBS, in which radiochemical purity kept over 96 % in 72 h.

3.2. Specific binding and uptake of ^{177}Lu-S1R/PSMA-P in LNCaP cells

It has been reported that over 40 % prostate cancer patients overexpress Sigma receptors [50] and 90 % overexpress PSMA [51]. Here, we firstly assessed the expression of Sigma receptors and PSMA in LNCaP cells by flow cytometry [52]. The results (Fig. 1e) demonstrated clear overexpression of both PSMA and Sigma-1 receptors in LNCaP cells, though PSMA was approximately ten times higher expression than Sigma-1 receptor. Interestingly, ^{177}Lu-S1R/PSMA-P revealed much stronger binding to LNCaP cells than single PSMA targeted control ^{177}Lu-PSMA-617 and moreover marked increase in binding over time (Fig. 1f). The binding activity of ^{177}Lu-S1R/PSMA-P was more than three times that of ^{177}Lu-PSMA-617 at 4 and 24 h of incubation. The markedly enhanced binding affinity of S1R/PSMA-P compared to PSMA-617 likely results from not only increased affinity to the cell surface but also improved uptake and retention inside cells by binding to the Sigma-1 receptor in the endoplasmic reticulum. It has been reported that binding to Sigma-1 receptor boosts endocytosis [44] and there are abundant Sigma-1 receptor in the endoplasmic reticulum [53,54]. The competitive experiments showed that binding of ^{177}Lu-S1R/PSMA-P by LNCaP cells was completely inhibited by 6.5 mM SIR/PSMA-P, supporting receptor-mediated uptake of ^{177}Lu-S1R/PSMA-P by LNCaP cells. Moreover, in PSMA-positive Sigma-1 receptor-negative RM1 cells, ^{177}Lu-S1R/PSMA-P showed similar uptake as ^{177}Lu-PSMA-617 (**Fig. S3**), certifying that Sigma-1 receptor does play a role.

3.3. Pharmacokinetics and biodistribution of ^{177}Lu/^{68}Ga -S1R/PSMA-P

The pharmacokinetics and biodistribution of ^{177}Lu-S1R/PSMA-P were investigated using *micro*SPECT/CT in LNCaP tumor-bearing mice and ^{177}Lu-PSMA-617 was used as a control. The images at different time points post-injection demonstrated superior tumor uptake and retention of ^{177}Lu-S1R/PSMA-P to ^{177}Lu-PSMA-617 (Fig. 2a, b). In contrast to fast weakening of ^{177}Lu signal in the tumor at 48 and 72 h post-injection of ^{177}Lu-PSMA-617, ^{177}Lu-S1R/PSMA-P kept practically the same strong ^{177}Lu signal in the tumor from 1 to 72 h. Importantly, ^{177}Lu-S1R/PSMA-P was rapidly excreted via the renal pathway and essentially no ^{177}Lu-S1R/PSMA-P was detected in other normal organs. The quantitative analyses of uptake by tumor and major organs revealed a remarkably high tumor level of 27.3 ± 2.8 % injection dose per volume (%ID/cc) for ^{177}Lu-S1R/PSMA-P at 4 h postinjection, which was about two-fold that of single PSMA-targeted control (Fig. 2c, d). ^{177}Lu-S1R/PSMA-P retained a high accumulation at the tumor throughout the whole observation period of time (1–72 h), and the area under the curve (AUC) of ^{177}Lu-S1R/PSMA-P was calculated to be 1680.0 ± 60.7 h•%ID/cc, which was approximately three-fold that of ^{177}Lu-PSMA-617 (Fig. 2e). As for ^{177}Lu-PSMA-617 and many other peptides, kidney is a major organ for metabolization [55]. Kidney toxicity is a major concern. Fig. 2f shows a fast excretion of ^{177}Lu-S1R/PSMA-P, similar to ^{177}Lu-PSMA-617, indicating a potentially low kidney toxicity. Fast glomerular filtration is possible due to the hydrophilicity of ^{177}Lu-S1R/PSMA-P and its molecular weight of 1708 Da [56]. The plot of tumor-to-normal tissue (T/N) ratio demonstrated clearly better selectivity of ^{177}Lu-S1R/PSMA-P to LNCaP tumor than single PSMA-targeted control, in which 4.8, 7.8, 1.2, and 1.6 times higher T/N ratio was observed in blood, liver, kidney and muscle, respectively (Fig. 2g). Albumin binding strategy increases tumor uptake, but also increases renal uptake and haematotoxicity [57]. A good radiopharmaceutical must balance tumor uptake, haematotoxicity, and renal distribution [2]. The PET images of ^{68}Ga-S1R/PSMA-P and ^{68}Ga-PSMA-617 further corroborated fast and selective homing of S1R/PSMA-P to LNCaP tumor (Fig. 2h, i). We noticed also a high uptake of ^{68}Ga-S1R/PSMA-P in the kidney. The tumor/kidney ratio for ^{177}Lu-S1R/PSMA-P is similar to PSMA-617. The high uptake in the tumor renders it better in identifying metastatic tumors, screening patients, and monitoring the treatment effects. In comparison, no tumor uptake of ^{177}Lu-S1R/PSMA-P was observed in PSMA-negative PC-3 tumor-bearing mouse model (Fig. 2j), signifying a high specificity of ^{177}Lu-S1R/PSMA-P toward PSMA receptor. The above results demonstrated that ^{177}Lu-S1R/PSMA-P has superior selectivity, uptake, and retention in LNCaP tumor to ^{177}Lu-PSMA-617 control.

To accurately evaluate its biodistribution behavior, mice at different time points (1, 4, 24, 72, and 168 h) post-injection of ^{177}Lu-S1R/PSMA-P were sacrificed and tumor and organs such as heart, liver, spleen, kidneys, and muscle were isolated and measured with radioactivity. The results confirmed a high selectivity of ^{177}Lu-S1R/PSMA-P toward LNCaP tumor (Fig. 3a). ^{177}Lu-S1R/PSMA-P exhibited a maximum tumor accumulation of 28.4 ± 4.9 % injection dose per gram (%ID/g) of tissue at 4 h post-injection and kept high even at 168 h post-injection (14.9 ± 4.7 % ID/g). Notably, except for kidney, all the other organs had essentially no

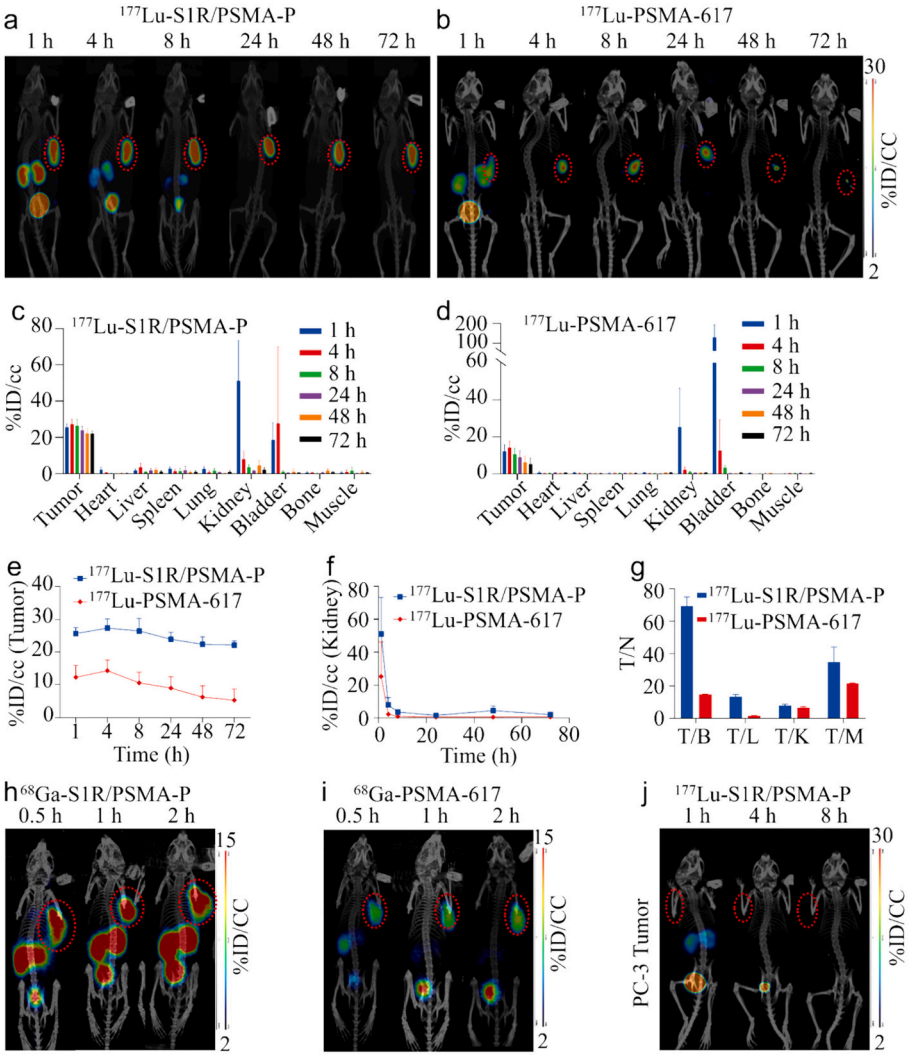

Fig. 2. SPECT/CT images of LNCaP tumor-bearing mice intravenously injected with ^{177}Lu-S1R/PSMA-P (7.4 MBq) (a) and ^{177}Lu-PSMA-617 (7.4 MBq) (b) ($n = 3$). The red dotted line shows the location of the tumor. Biodistribution of ^{177}Lu-S1R/PSMA-P (c) and ^{177}Lu-PSMA-617 (d) quantified from SPECT images. Accumulation of ^{177}Lu-S1R/PSMA-P and ^{177}Lu-PSMA-617 in tumor (e) and kidney (f). (g) Tumor-to-normal tissue (T/N) ratio of ^{177}Lu-S1R/PSMA-P and ^{177}Lu-PSMA-617. T/B: tumor to blood, T/L: tumor to liver, T/K: tumor to kidney, T/M: tumor to muscle. PET/CT images of LNCaP tumor-bearing mice intravenously injected with ^{68}Ga-S1R/PSMA-P (3.7 MBq) (h) and ^{68}Ga-PSMA-617 (3.7 MBq) (i) (n = 3). (j) SPECT/CT images of PC3 tumor-bearing mice intravenously injected with ^{177}Lu-S1R/PSMA-P (7.4 MBq) (n = 3). (For interpretation of the references to colour in this figure legend, the reader is referred to the web version of this article.)

or low accumulation of ^{177}Lu (< 1 %ID/g) after 4 h post-injection. The kidney level of ^{177}Lu-S1R/PSMA-P reduced to less than 6 %ID/g after 24 h post-injection. It should be noted that unlike marked expression of PSMA in mouse kidneys, human kidneys have only moderate PSMA expression [57,58]. ^{177}Lu-S1R/PSMA-P will not likely cause significant kidney toxicity in patients.

The pharmacokinetics of ^{177}Lu-S1R/PSMA-P was studied in healthy male BALB/c. The results showed fast elimination of ^{177}Lu-S1R/PSMA-P with a half-life of 0.16 h, which is comparable to that of ^{177}Lu-PSMA-617 (0.15 h) (Fig. 3b**).** This rapid excretion is beneficial as it may effectively reduce off-target toxicity [59,60].

3.4. Radionuclide therapy of prostate tumor

The in vivo antitumor efficacy of ^{177}Lu-S1R/PSMA-P was conducted in LNCaP-FGC tumor-bearing mice. The mice with tumor volume of about 400 mm^3 were randomly divided into five groups ($n = 10$) and intravenously injected with PBS, ^{177}Lu-PSMA-617 control at 33.3 MBq, and ^{177}Lu-S1R/PSMA-P with low, medium, and high doses (3.7 MBq, 11.1 MBq, and 33.3 MBq) to see the effect of dosage. Fig. 4a demonstrates that a single dose of ^{177}Lu-S1R/PSMA-P effectively inhibited tumor growth and the antitumor efficacy was clearly dose-dependent. Interestingly, ^{177}Lu-S1R/PSMA-P at a very low dose of 3.7 MBq induced better tumor inhibition than single-targeted control at 33.3 MBq. Reducing the administration dose not only ensures patient safety, but also reduces the financial burden on the patient [61]. ^{177}Lu-S1R/PSMA-P at both 11.1 and 33.3 MBq brought about continuous and pronounced shrinkage of tumor over 21 days post injection, in which tumor volumes decreased from about 400 mm^3 to 217.4 ± 78.9 mm^3 and 122.3 ± 29.5 mm^3, respectively. On day 21 post injection, all mice were euthanized, and the tumors were collected, weighted, and photographed (Fig. 4b). Tumor growth inhibition (TGI) was calculated according to the tumor weight. The TGI of ^{177}Lu-S1R/PSMA-P at dose of 11.1 and 33.3 MBq was 88.3 ± 5.5 % and 94.2 ± 2.8 %, respectively, while single-targeted control was only 38.2 ± 29.4 % (Fig. 4c). Little body weight loss was observed in all the groups during the whole treatment period (Fig. 4d), which is in line with excellent targetability and fast excretion of ^{177}Lu-S1R/PSMA-P. The results confirmed superior tumor inhibitory effect of ^{177}Lu-S1R/PSMA-P to single-targeted control.

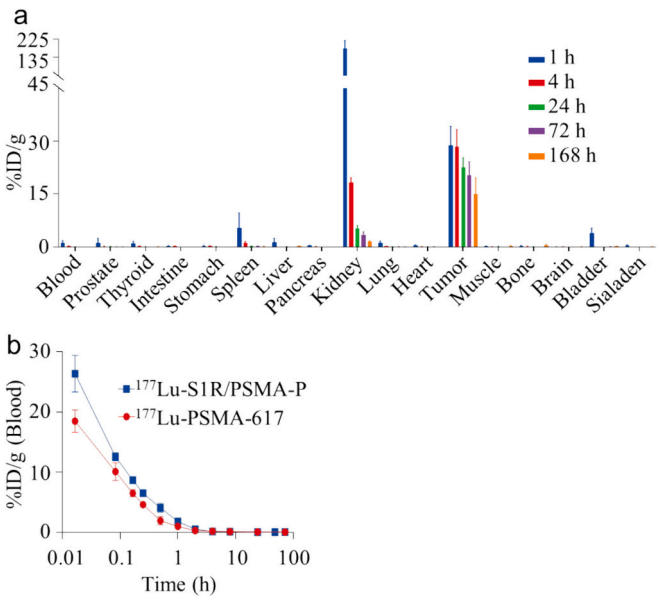

Fig. 3. (a) The biodistribution of ^{177}Lu-S1R/PSMA-P (7.4 MBq) in LNCaP tumor-bearing mice at different times post injection (n = 3). The mice were sacrificed at 1, 4, 24, 72, and 168 h post injection, the organs were isolated, and the radioactivity was measured by gamma counter. (b) The pharmacokinetics of ^{177}Lu-S1R/PSMA-P and ^{177}Lu-PSMA-617 in healthy male BALB/c mice following intravenous injection (1.85 MBq) (n = 4).

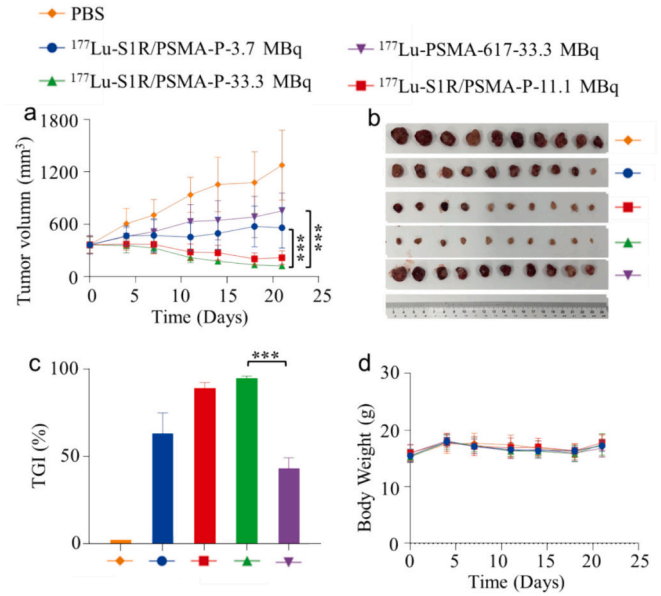

Fig. 4. In vivo antitumor performance of a single injection of ^{177}Lu-S1R/PSMA-P (3.7 MBq, 11.1 MBq, and 33.3 MBq) and ^{177}Lu-PSMA-617 (33.3 MBq) in LNCaP-FGC tumor-bearing mice (n = 10). (a) Tumor volume change over time. (b) The photograph of the tumor on the 21st day of treatment. (c) Mean tumor inhibition rate. (d) Body weight change of mice. P values were calculated by One-way ANOVA with Tukey multiple comparison tests, p* <0.05, p** <0.01, p*** <0.001.

3.5. Safety assessment of ^{177}Lu-S1R/PSMA-P

The safety of ^{177}Lu-S1R/PSMA-P was further assessed in healthy BALB/c mice and male rats. As shown above, ^{177}Lu-S1R/PSMA-P at a low dosage of 3.7 MBq is already better than ^{77}Lu-PSMA-517 at 33.3 MBq. The toxicology assessment of ^{177}Lu-S1R/PSMA-P was then carried out at escalating doses of 2 and 4-fold with respect to 3.7 MBq. The blood tests after intravenous injection of 7.4 MBq or 14.8 MBq of ^{177}Lu-S1R/PSMA-P demonstrated that blood parameters, including white blood cells, red blood cells, and platelets of mice were all at normal levels (Fig. 5a). Given the low toxicity observed in the blood analysis, we further escalated the doses in the toxicology assessment based on bodyweight to 4 and 8-fold. The monitoring of mouse body weights following intravenous injection of 14.8 MBq or 29.6 MBq of ^{177}Lu-S1R/PSMA-P displayed no significant change of body weight over 27 days (Fig. 5b). On day 27, the mice were sacrificed, and major organs were harvested and sliced for hematoxylin and eosin (H&E) staining. The results showed no tissue abnormalities in all organs including heart, liver, spleen, lung, and kidney (Fig. 5c). The blood tests at 4 days post intravenous injection of ^{177}Lu-S1R/PSMA-P in male rats at a dose of 185 MBq or 370 MBq, which is comparable to the clinically intended maximum dose of 123.3 MBq/kg, showed normal hemogram, blood biochemical parameters (Fig. 5d), and no tissue abnormalities in any organs (**Fig. S4**). All the above results point out that ^{177}Lu-S1R/PSMA-P presents an excellent safety profile.

Our findings show that PSMA and Sigma-1 receptor dual-targeted peptide while greatly enhancing the uptake and retention in LNCaP prostate tumor in mice does not sacrifice the selectivity, as revealed by a higher T/N ratio of ^{177}Lu-S1R/PSMA-P in nearly all normal organs and blood than ^{177}Lu-PSMA-617. It should further be noted that ^{177}Lu-S1R/PSMA-P has a similar pharmacokinetics to single-targeted control and is quickly excreted by the kidney. This augmented tumor-selectivity of ^{177}Lu-S1R/PSMA-P signifies that both PSMA and Sigma-1 receptor are highly specific and minimally expressed on the surface of healthy cells. The superior tumor retention of ^{177}Lu-S1R/PSMA-P is most likely due to its binding to the Sigma-1 receptor in the endoplasmic reticulum following receptor-mediated uptake, which circumvents detachment and tumor clearance. The retention plays a key role in tumor targetability and efficacy. Li et al. recently reported that covalent chemical ligation following peptide-mediated specific cell binding effectively prevented dissociation of radiopharmaceuticals, leading to elevated cell binding, augmented tumor uptake and prolonged tumor retention [62]. For nanomedicines, quick dissociation and tumor clearance are also among the major reasons for lessened tumor accretion and inadequate tumor retention. Our preliminary clinical studies showed that ^{177}Lu-S1R/PSMA-P at a low dosage of 120 mCi, which is nearly half of that for ^{177}Lu-PSMA-617, brought about effective radioligand therapy of metastatic castration-resistant prostate cancer (mCRPC) patients, without causing unmanageable adverse effects, validating its clinical advantages. In addition to being overexpressed in prostate cancer cells, PSMA is also overexpressed in the neovasculature of malignant tumors such as gastric cancer, breast cancer, and lung cancer [63–65], which makes ^{177}Lu-S1R/PSMA-P potentially interesting for radioligand therapy of different tumors.

4. Conclusion

We have demonstrated that Sigma-1 receptor and PSMA dual-receptor targeted peptide (S1R/PSMA-P) mediates high-efficacy radionuclide imaging and therapy of LNCaP prostate tumor in mice. ^{177}Lu-S1R/PSMA-P holds several unique features: (i) it has a high specific activity and radiostability; (ii) it exhibits markedly enhanced affinity to LNCaP cells over single-targeted control ^{177}Lu-PSMA-617; (iii) it shows exceptional uptake and retention in LNCaP tumor, affording not only about 2-fold better tumor accumulation but also higher tumor selectivity than PSMA single-targeted control; (iv) it has a low distribution in healthy organs and is quickly excreted via kidney; and (v) it has little systemic toxicity. As a result, ^{177}Lu-S1R/PSMA-P induces far superior inhibitory effect toward LNCaP prostate tumor in mice to single-targeted control. Notably, ^{68}Ga-S1R/PSMA-P with a high tumor selectivity gives clear PET imaging of LNCaP tumor at 0.5 to 2 h post injection, rendering S1R/PSMA-P also interesting for diagnosis, patient screening, and

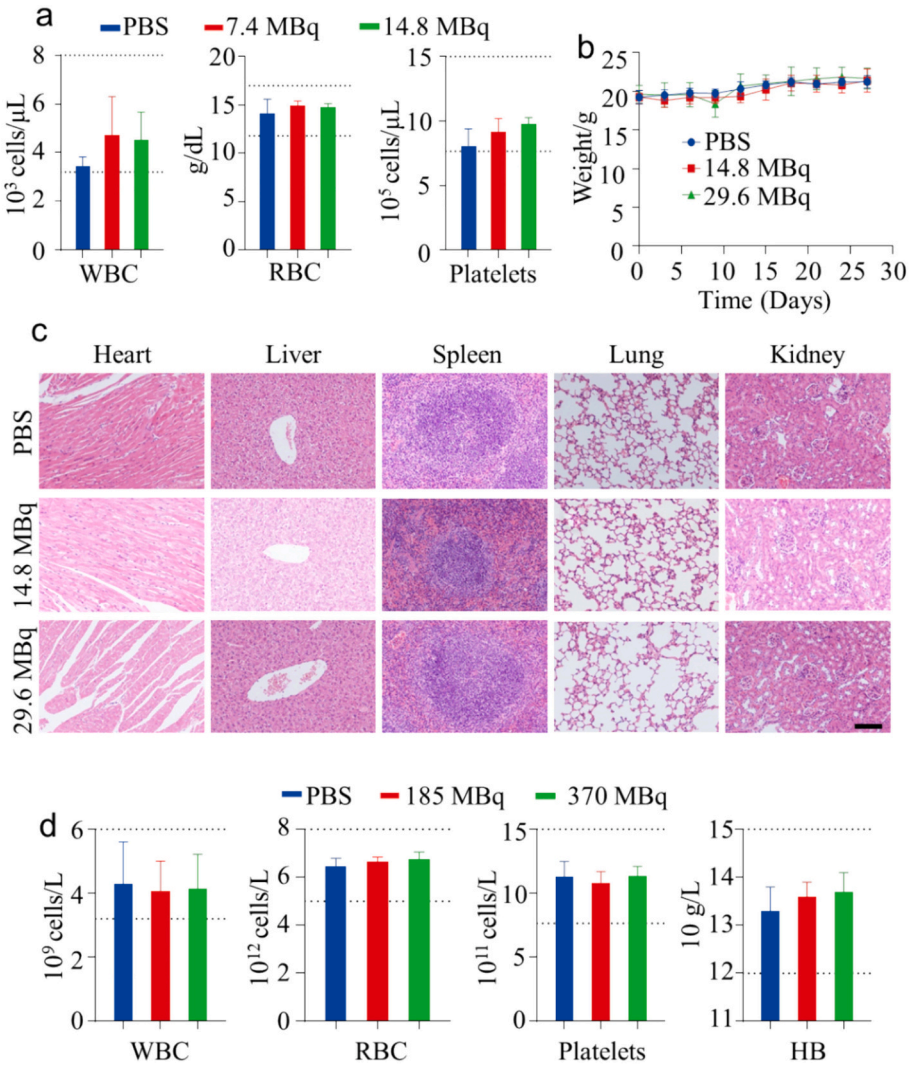

Fig. 5. Blood cells change (a) and body weight change (b) of mice after intravenous injection of ^{177}Lu-S1R/PSMA-P ($n = 5$). (c) Microscopic images of H&E stained organs in healthy mice after intravenous injection of ^{177}Lu-S1R/PSMA-P excised on day 27 (n = 5). The scale bar corresponds to 100 μm. (d) Blood cells change of SD male rats after intravenous injection of ^{177}Lu-S1R/PSMA-P ($n = 10$). WBC: white blood cell, RBC: red blood cells, HB: hemoglobin index. (For interpretation of the references to colour in this figure legend, the reader is referred to the web version of this article.)

monitoring of treatment effects. ^{68}Ga/^{177}Lu-S1R/PSMA-P is currently under clinical studies for the screening and treatment of metastatic castration-resistant prostate cancer (mCRPC) patients. This novel dual receptor-targeted peptide, with improved selectivity and safety, presents an appealing radionuclide therapy for malignant tumors.

CRediT authorship contribution statement

Zhenyuan Huangfu: Writing – original draft, Investigation, Formal analysis, Data curation, Conceptualization. **Jiangtao Yang:** Validation, Project administration, Investigation, Formal analysis, Data curation. **Juan Sun:** Writing – original draft, Methodology, Investigation, Formal analysis, Data curation. **Bin Xu:** Methodology, Investigation, Formal analysis, Data curation. **Lei Tao:** Methodology, Investigation, Formal analysis, Data curation. **Jiang Wu:** Investigation, Formal analysis, Data curation, Conceptualization. **Feng Wang:** Writing – review & editing, Validation, Resources, Datat curation, Conceptualization. **Guanglin Wang:** Writing – review & editing, Validation, Supervision, Resources, Data curation, Conceptualization. **Fenghua Meng:** Supervision, Resources, Project administration, Investigation. **Zhiyuan Zhong:** Writing – review & editing, Writing – original draft, Supervision, Funding acquisition, Conceptualization.

Declaration of competing interest

The authors declare no competing financial interest.

Data availability

Data will be made available on request.

Acknowledgments

This work is supported by research grants from the National Natural Science Foundation of China (52033006, 52233007).

References

[1] M. Senior, Precision radiation opens a new window on cancer therapy, Nat. Biotechnol. (2024) 1–6.
[2] L. Bodei, K. Herrmann, H. Schoder, A.M. Scott, J.S. Lewis, Radiotheranostics in oncology: current challenges and emerging opportunities, Nat. Rev. Clin. Oncol. 19 (2022) 534–550.
[3] K. Herrmann, M. Schwaiger, J.S. Lewis, S.B. Solomon, B.J. McNeil, M. Baumann, S. S. Gambhir, H. Hricak, R. Weissleder, Radiotheranostics: a roadmap for future development, Lancet Oncol. 21 (2020) e146–e156.

[4] G. Sgouros, L. Bodei, M.R. McDevitt, J.R. Nedrow, Radiopharmaceutical therapy in cancer: clinical advances and challenges, Nat. Rev. Drug Discov. 19 (2020) 589–608.
[5] S. Banerjee, M.R. Pillai, F.F. Knapp, Lutetium-177 therapeutic radiopharmaceuticals: linking chemistry, radiochemistry, and practical applications, Chem. Rev. 115 (2015) 2934–2974.
[6] K.A. Morgan, S.E. Rudd, A. Noor, P.S. Donnelly, Theranostic nuclear medicine with gallium-68, lutetium-177, copper-64/67, actinium-225, and lead-212/203 radionuclides, Chem. Rev. 123 (2023) 12004–12035.
[7] H.J. Wester, M. Schottelius, PSMA-targeted radiopharmaceuticals for imaging and therapy, Semin. Nucl. Med. 49 (2019) 302–312.
[8] A. Farolfi, G.M. Lima, W. Oyen, S. Fanti, Molecular imaging and theranostics-a multidisciplinary approach, Semin. Nucl. Med. 49 (2019) 247–254.
[9] J. Sun, Z. Huangfu, J. Yang, G. Wang, K. Hu, M. Gao, Z. Zhong, Imaging-guided targeted radionuclide tumor therapy: from concept to clinical translation, Adv. Drug Deliv. Rev. 190 (2022) 114–538.
[10] J. Chau, N. Yu, H. Bakeri, Y. Menda, J.S. Dillon, C. Chandrasekharan, Real-world analysis of peptide receptor radionuclide therapy (PRRT) in the treatment of neuroendocrine tumors, J. Clin. Oncol. 38 (2020) e16701.
[11] G. di Santo, G. Santo, A. Sviridenko, I. Virgolini, Peptide receptor radionuclide therapy combinations for neuroendocrine tumours in ongoing clinical trials: status 2023, Theranostics 14 (2024) 940–953.
[12] K. Rahbar, A. Bode, M. Weckesser, N. Avramovic, M. Claesener, L. Stegger, M. Bögemann, Radioligand therapy with ^{177}Lu-PSMA-617 as a novel therapeutic option in patients with metastatic castration resistant prostate cancer, Clin. Nucl. Med. 41 (2016) 522–528.
[13] J. Strosberg, G. El-Haddad, E. Wolin, A. Hendifar, J. Yao, B. Chasen, E. Mittra, P. L. Kunz, M.H. Kulke, H. Jacene, D. Bushnell, T.M. O'Dorisio, R.P. Baum, H. R. Kulkarni, M. Caplin, R. Lebtahi, T. Hobday, E. Delpassand, E. Van Cutsem, A. Benson, R. Srirajaskanthan, M. Pavel, J. Mora, J. Berlin, E. Grande, N. Reed, E. Seregni, K. Oberg, M.L. Sierra, P. Santoro, T. Thevenet, J.L. Erion, P. Ruszniewski, D. Kwekkeboom, E. Krenning, N.-T. Investigators, Phase 3 trial of ^{177}Lu-Dotatate for midgut neuroendocrine tumors, New Engl. J. Med. 376 (2017) 125–135.
[14] M.P. Yadav, S. Ballal, R.K. Sahoo, S.N. Dwivedi, C. Bal, Radioligand therapy with ^{177}Lu-PSMA for metastatic castration-resistant prostate cancer: a systematic review and meta-analysis, Am. J. Roentgenol. 213 (2019) 275–285.
[15] K. Jewell, M.S. Hofman, J.S.L. Ong, S. Levy, Emerging theranostics for prostate cancer and a model of prostate-specific membrane antigen therapy, Radiology 311 (2024) e231703.
[16] M.S. Hofman, L. Emmett, S. Sandhu, A. Iravani, J.P. Buteau, A.M. Joshua, J.C. Goh, D.A. Pattison, T.H. Tan, I.D. Kirkwood, S. Ng, R.J. Francis, C. Gedye, N. K. Rutherford, A. Weickhardt, A.M. Scott, S.-T. Lee, E.M. Kwan, A.A. Azad, S. Ramdave, A.D. Redfern, W. Macdonald, A. Guminski, E. Hsiao, W. Chua, P. Lin, A.Y. Zhang, M.R. Stockler, S.G. Williams, A.J. Martin, I.D. Davis, T. Akhurst, R. Alipour, D. Bailey, P. Banks, A. Beaulieu, L. Campbell, M. Crumbaker, N. Dhiantravan, A. Hamid, M. Haskali, T. Hung, G. Kong, N. Lawrence, J. Lewin, M. McCarthy, K. Moodie, D. Murphy, A. Nguyen, D. Pook, A. Ravi Kumar, P. Roach, P. Roselt, J. Saghebi, G. Schembri, L. Spain, S. Subramaniam, S.P. Thang, P. Thomas, B. Tran, R. Wallace, S. Yip, Overall survival with ^{177}Lu-PSMA-617 versus cabazitaxel in metastatic castration-resistant prostate cancer (TheraP): secondary outcomes of a randomized, open-label, phase 2 trial, Lancet Oncol. 25 (2024) 99–107.
[17] O. Sartor, J. de Bono, K.N. Chi, K. Fizazi, K. Herrmann, K. Rahbar, S.T. Tagawa, L. T. Nordquist, N. Vaishampayan, G. El-Haddad, C.H. Park, T.M. Beer, A. Armour, W. J. Pérez-Contreras, M. DeSilvio, E. Kpamegan, G. Gericke, R.A. Messmann, M. J. Morris, B.J. Krause, V. Investigators, Lutetium-177-PSMA-617 for metastatic castration-resistant prostate cancer, New Engl. J. Med. 385 (2021) 1091–1103.
[18] L.M. Unterrainer, J. Calais, N.H. Bander, Prostate-specific membrane antigen: gateway to management of advanced prostate cancer, Annu. Rev. Med. 75 (2024) 49–66.
[19] T. Maurer, M. Eiber, M. Schwaiger, J.E. Gschwend, Current use of PSMA-PET in prostate cancer management, Nat. Rev. Urol. 13 (2016) 226–235.
[20] A.S. Ravi Kumar, M.S. Hofman, Mechanistic insights for optimizing PSMA radioligand therapy, Clin. Cancer Res. 26 (2020) 2774–2776.
[21] Z. Wang, R. Tian, G. Niu, Y. Ma, L. Lang, L.P. Szajek, D.O. Kiesewetter, O. Jacobson, X. Chen, Single low-dose injection of Evans blue modified PSMA-617 radioligand therapy eliminates prostate-specific membrane antigen positive tumors, Bioconjug. Chem. 29 (2018) 3213–3221.
[22] L.M. Deberle, M. Benesova, C.A. Umbricht, F. Borgna, M. Buchler, K. Zhernosekov, R. Schibli, C. Muller, Development of a new class of PSMA radioligands comprising ibuprofen as an albumin-binding entity, Theranostics 10 (2020) 1678–1693.
[23] H.T. Kuo, H. Merkens, Z. Zhang, C.F. Uribe, J. Lau, C. Zhang, N. Colpo, K.S. Lin, F. Benard, Enhancing treatment efficacy of ^{177}Lu-PSMA-617 with the conjugation of an abumin-binding motif: preclinical dosimetry and endoradiotherapy studies, Mol. Pharm. 15 (2018) 5183–5191.
[24] H. Hou, Y. Pan, Y. Wang, Y. Ma, X. Niu, S. Sun, G. Hou, W. Tao, F. Gao, Development and first-in-human study of PSMA-targeted PET tracers with improved pharmacokinetic properties, Eur. J. Nucl. Med. Mol. Imaging (2024) 1–14.
[25] X. Wen, P. Xu, X. Zeng, J. Liu, C. Du, X. Zeng, X. Cheng, X. Wang, Y. Liang, T. Zhao, H. Yang, H. Li, L. Meng, J. Fang, H. Liu, Z. Zhou, J. Zhang, X. Zhang, Z. Guo, X. Chen, Development of ^{177}Lu-LNC1003 for radioligand therapy of prostate cancer with a moderate level of PSMA expression, Eur. J. Nucl. Med. Mol. Imaging 50 (2023) 2846–2860.
[26] D. Pilati, K.A. Howard, Albumin-based drug designs for pharmacokinetic modulation, Expert. Opin. Drug. Met. 16 (2020) 783–795.
[27] J.M. Kelly, A. Amor-Coarasa, S. Ponnala, A. Nikolopoulou, C. Williams Jr., S. G. DiMagno, J.W. Babich, Albumin-binding PSMA ligands: implications for expanding the therapeutic window, J. Nucl. Med. 60 (2019) 656–663.
[28] V.J. Tschan, S.D. Busslinger, P. Bernhardt, P.V. Grundler, J.R. Zeevaart, U. Köster, N.P.V.D. Meulen, R. Schibli, C. Müller, Albumin-binding and conventional PSMA ligands in combination with ^{161}Tb: biodistribution, dosimetry, and preclinical therapy, J. Nucl. Med. 64 (2023) 1625–1631.
[29] J. Kelly, A. Amor-Coarasa, S. Ponnala, A. Nikolopoulou, C. Williams Jr., D. Schlyer, Y. Zhao, D. Kim, J.W. Babich, Trifunctional PSMA-targeting constructs for prostate cancer with unprecedented localization to LNCaP tumors, Eur. J. Nucl. Med. Mol. Imaging 45 (2018) 1841–1851.
[30] B. Yu, H. Wei, Q. He, C.A. Ferreira, C.J. Kutyreff, D. Ni, Z.T. Rosenkrans, L. Cheng, F. Yu, J.W. Engle, X. Lan, W. Cai, Efficient uptake of ^{177}Lu-porphyrin-PEG nanocomplexes by tumor mitochondria for multimodal-imaging-guided combination therapy, Angew. Chem. Int. Ed. Eng. 57 (2018) 218–222.
[31] M. Benesova, U. Bauder-Wust, M. Schafer, K.D. Klika, W. Mier, U. Haberkorn, K. Kopka, M. Eder, Linker modification strategies to control the prostate-specific membrane antigen (PSMA)-targeting and pharmacokinetic properties of DOTA-conjugated PSMA inhibitors, J. Med. Chem. 59 (2016) 1761–1775.
[32] N. Meher, G.W. Ashley, K.N. Bobba, A. Wadhwa, A.P. Bidkar, C. Dasari, C. Mu, R. A. Sankaranarayanan, J.A.C. Serrano, A. Raveendran, D.P. Bulkley, R. Aggarwal, N. Y. Greenland, A. Oskowitz, D.M. Wilson, Y. Seo, D.V. Santi, H.F. VanBrocklin, R. R. Flavell, Prostate-specific membrane antigen targeted starPEG nanocarrier for imaging and therapy of prostate cancer, Adv. Healthc Mater, n/a 2304618 (2024).
[33] W. Yan, B. Guo, Z. Wang, J. Yang, Z. Zhong, F. Meng, RGD-directed 24 nm micellar docetaxel enables elevated tumor-liver ratio, deep tumor penetration and potent suppression of solid tumors, J. Control. Release 360 (2023) 304–315.
[34] C.A. Umbricht, M. Benesova, R. Schibli, C. Muller, Preclinical development of novel PSMA-targeting radioligands: modulation of albumin-binding properties to improve prostate cancer therapy, Mol. Pharm. 15 (2018) 2297–2306.
[35] A.A. Uspenskaya, E.A. Nimenko, R.R. Shafikov, N.Y. Zyk, S.A. Evteev, N. S. Dashkova, Y.A. Ivanenkov, A.G. Majouga, D.A. Skvortsov, A.S. Garanina, E. K. Beloglazkina, A.E. Machulkin, Optimization of the dipeptide motifs in the PSMA ligands linker structure: synthesis and in vitro evaluation, Med. Chem. Res. 32 (2023) 32–37.
[36] K. Durkan, Z. Jiang, T.L. Rold, G.L. Sieckman, T.J. Hoffman, R.P. Bandari, A. F. Szczodroski, L. Liu, Y. Miao, T.S. Reynolds, C.J. Smith, A heterodimeric [RGD-Glu-[^{64}Cu-NO$_2$A]-6-Ahx-RM2] alphavbeta3/GRPr-targeting antagonist radiotracer for PET imaging of prostate tumors, Nucl. Med. Biol. 41 (2014) 133–139.
[37] M. Eder, M. Schafer, U. Bauder-Wust, U. Haberkorn, M. Eisenhut, K. Kopka, Preclinical evaluation of a bispecific low-molecular heterodimer targeting both PSMA and GRPR for improved PET imaging and therapy of prostate cancer, Prostate 74 (2014) 659–668.
[38] K. Hu, L. Li, Y. Huang, S. Ye, J. Zhong, Q. Yan, Y. Zhong, L. Fu, P. Feng, H. Li, Radiosynthesis and preclinical evaluation of bispecific PSMA/FAP heterodimers for tumor imaging, Pharmaceuticals 15 (2022) 383.
[39] A. Abouzayed, C.B. Yim, B. Mitran, S.S. Rinne, V. Tolmachev, M. Larhed, U. Rosenstrom, A. Orlova, Synthesis and preclinical evaluation of radio-iodinated GRPR/PSMA bispecific heterodimers for the theranostics application in prostate cancer, Pharmaceutics 11 (2019) 357.
[40] A. Verena, Z. Zhang, H.-T. Kuo, H. Merkens, J. Zeisler, R. Wilson, S. Bendre, A.A.W. L. Wong, F. Bénard, K.-S. Lin, Synthesis and preclinical evaluation of three novel ^{68}Ga-labeled bispecific PSMA/FAP-targeting tracers for prostate cancer imaging, Molecules 28 (2023) 1088.
[41] E.J. Cobos, J.M. Entrena, F.R. Nieto, C.M. Cendán, E. Del Pozo, Pharmacology and therapeutic potential of sigma$_1$ receptor ligands, Curr. Neuropharmacol. 6 (2008) 344–366.
[42] N.A. Colabufo, C. Abate, M. Contino, C. Inglese, M. Niso, F. Berardi, R. Perrone, PB183, a sigma receptor ligand, as a potential PET probe for the imaging of prostate adenocarcinoma, Bioorg. Med. Chem. Lett. 18 (2008) 1990–1993.
[43] V. Megalizzi, M. Le Mercier, C. Decaestecker, Sigma receptors and their ligands in cancer biology: overview and new perspectives for cancer therapy, Med. Res. Rev. 32 (2012) 410–427.
[44] A. van Waarde, A.A. Rybczynska, N.K. Ramakrishnan, K. Ishiwata, P.H. Elsinga, R. A. Dierckx, Potential applications for sigma receptor ligands in cancer diagnosis and therapy, Biochim. Biophys. Acta 2015 (1848) 2703–2714.
[45] J.D. Thomas, C.G. Longen, H.M. Oyer, N. Chen, C.M. Maher, J.M. Salvino, B. Kania, K.N. Anderson, W.F. Ostrander, K.E. Knudsen, F.J. Kim, Sigma1 targeting to suppress aberrant androgen receptor signaling in prostate cancer, Cancer Res. 77 (2017) 2439–2452.
[46] B. Shen, D. Yoon, J. Castillo, S. Biswal, A practical guide to sigma-1 receptor positron emission tomography/magnetic resonance imaging: a new clinical molecular imaging method to identify peripheral pain generators in patients with chronic pain, Semin. Musculoskelet. Radiol. 27 (2023) 601–617.
[47] J. Guo, J.R. Ogier, S. Desgranges, R. Darcy, C. O'Driscoll, Anisamide-targeted cyclodextrin nanoparticles for siRNA delivery to prostate tumours in mice, Biomaterials 33 (2012) 7775–7784.
[48] K.A. Fitzgerald, M. Malhotra, M. Gooding, F. Sallas, J.C. Evans, R. Darcy, C. M. O'Driscoll, A novel, anisamide-targeted cyclodextrin nanoformulation for siRNA delivery to prostate cancer cells expressing the sigma-1 receptor, Int. J. Pharm. 499 (2016) 131–145.
[49] K.A. Fitzgerald, K. Rahme, J. Guo, J.D. Holmes, C.M. O'Driscoll, Anisamide-targeted gold nanoparticles for siRNA delivery in prostate cancer – synthesis,

physicochemical characterisation and in vitro evaluation, J. Mater. Chem. B 4 (2016) 2242–2252.
[50] A. Dasargyri, C.D. Kumin, J.C. Leroux, Targeting nanocarriers with anisamide: fact or artifact? Adv. Mater. 29 (2017) 1603451.
[51] H. Zhang, S. Koumna, F. Pouliot, J.M. Beauregard, M. Kolinsky, PSMA theranostics: current landscape and future outlook, Cancers (Basel) 13 (2021) 4023.
[52] J. Jiang, R. Wang, L. Yang, Y. Sha, S. Zhao, J. Guo, D. Chen, Z. Zhong, F. Meng, IL-11Ralpha-targeted nanostrategy empowers chemotherapy of relapsed and patient-derived osteosarcoma, J. Control. Release 350 (2022) 460–470.
[53] B.J. Vilner, C.S. John, W.D. Bowen, Sigma-1 and Sigma-2 receptors are expressed in a wide variety of human and rodent tumor cell lines, Cancer Res. 55 (1995) 408–413.
[54] E. Aydar, P. Onganer, R. Perrett, M.B. Djamgoz, C.P. Palmer, The expression and functional characterization of sigma (sigma) 1 receptors in breast cancer cell lines, Cancer Lett. 242 (2006) 245–257.
[55] U. Hennrich, K. Kopka, Lutathera®: the first FDA- and EMA-approved radiopharmaceutical for peptide receptor radionuclide therapy, Pharmaceuticals 12 (2019) 114.
[56] E.A. Park, S.A. Graves, Y. Menda, The impact of radiopharmaceutical therapy on renal function, Semin. Nucl. Med. 52 (2022) 467–474.
[57] H.T. Kuo, K.S. Lin, Z. Zhang, C.F. Uribe, H. Merkens, C. Zhang, F. Benard, Novel ^{177}Lu-labeled albumin-binder-conjugated PSMA-targeting agents with extremely high tumor uptake and enhanced tumor-to-kidney absorbed dose ratio, J. Nucl. Med. 62 (2020) 521–527.
[58] M. Perera, N. Papa, D. Christidis, D. Wetherell, M.S. Hofman, D.G. Murphy, D. Bolton, N. Lawrentschuk, Sensitivity, specificity, and predictors of positive ^{68}Ga-prostate-specific membrane antigen positron emission tomography in advanced prostate cancer: a systematic review and meta-analysis, Eur. Urol. 70 (2016) 926–937.
[59] T.M. Kalidindi, S.G. Lee, K. Jou, G. Chakraborty, M. Skafida, S.T. Tagawa, N. H. Bander, H. Schoder, L. Bodei, N. Pandit-Taskar, J.S. Lewis, S.M. Larson, J. R. Osborne, N.V.K. Pillarsetty, A simple strategy to reduce the salivary gland and kidney uptake of PSMA-targeting small molecule radiopharmaceuticals, Eur. J. Nucl. Med. Mol. Imaging 48 (2021) 2642–2651.
[60] M. Meckel, V. Kubíček, P. Hermann, M. Miederer, F. Rösch, A DOTA based bisphosphonate with an albumin binding moiety for delayed body clearance for bone targeting, Nucl. Med. Biol. 43 (2016) 670–678.
[61] C.S. Cutler, Economics of new molecular targeted personalized radiopharmaceuticals, Semin. Nucl. Med. 49 (2019) 450–457.
[62] X.-Y. Cui, Z. Li, Z. Kong, Y. Liu, H. Meng, Z. Wen, C. Wang, J. Chen, M. Xu, Y. Li, J. Gao, W. Zhu, Z. Hao, L. Huo, S. Liu, Z. Yang, Z. Liu, Covalent targeted radioligands potentiate radionuclide therapy, Nature 630 (2024) 206–213.
[63] M. Kasoha, C. Unger, E. Solomayer, R. Bohle, C. Zaharia, F. Khreich, S. Wagenpfeil, I. Juhasz-Böss, Prostate-specific membrane antigen (PSMA) expression in breast cancer and its metastases, Clin. Exp. Metastasis 34 (2017) 479–490.
[64] L. Chen, S. Zou, D. Li, J. Zhou, Z. Cheng, J. Zhao, Y. Zhu, D. Kuang, X. Zhu, Prostate-specific membrane antigen expression in hepatocellular carcinoma, cholangiocarcinoma, and liver cirrhosis, World J. Gastroenterol. 26 (2020) 7664–7678.
[65] H.L. Wang, S.S. Wang, W.H. Song, Y. Pan, H.P. Yu, T.G. Si, Y. Liu, X.N. Cui, Z. Guo, Expression of prostate-specific membrane antigen in lung cancer cells and tumor neovasculature endothelial cells and its clinical significance, PLoS One 10 (2015) e0125924.